

Unsupervised Segmentation of Lungs from Chest Radiographs

Payel Ghosh, Sameer K. Antani, L. Rodney Long, George R. Thoma
Lister Hill Center for Biomedical Communications
U. S. National Library of Medicine
National Institutes of Health, Bethesda, MD

ABSTRACT

This paper describes our preliminary investigations for deriving and characterizing coarse-level textural regions present in the lung field on chest radiographs using unsupervised grow-cut (UGC), a cellular automaton based unsupervised segmentation technique. The segmentation has been performed on a publicly available data set of chest radiographs. The algorithm is useful for this application because it automatically converges to a natural segmentation of the image from random seed points using low-level image features such as pixel intensity values and texture features.

Our goal is to develop a portable screening system for early detection of lung diseases for use in remote areas in developing countries. This involves developing automated algorithms for screening x-rays as normal/abnormal with a high degree of sensitivity, and identifying lung disease patterns on chest x-rays. Automatically deriving and quantitatively characterizing abnormal regions present in the lung field is the first step toward this goal. Therefore, region-based features such as geometrical and pixel-value measurements were derived from the segmented lung fields. In the future, feature selection and classification will be performed to identify pathological conditions such as pulmonary tuberculosis on chest radiographs. Shape-based features will also be incorporated to account for occlusions of the lung field and by other anatomical structures such as the heart and diaphragm.

Keywords: Chest radiographs, Segmentation, Region characterization, Cellular automata.

1. INTRODUCTION

The Lister Hill National Center for Biomedical Communications (LHNBC) of the National Library of Medicine (NLM) in collaboration with AMPATH (Academic Model Providing Access to Healthcare), the largest AIDS treatment program in the third world is working to develop a portable digital chest x-ray and automatic screening system for remote areas in developing countries. Portable computer-aided diagnosis systems have the potential to improve patient survival rates in remote areas where people do not have easy access to medical facilities. Our broader goal is to develop automated algorithms for screening x-rays and identifying pathological conditions on chest x-rays with a high degree of sensitivity.

Digital x-rays are commonly used to assess patients with lung diseases, such as lung cancer, tuberculosis, and interstitial lung disease. Accurately identifying subtle lung disease patterns from chest radiographs with high sensitivity is a challenging problem due to low contrast and superimposed anatomical structures. Several computer-aided diagnosis (CAD) schemes have been proposed in the literature to automatically detect and quantify pathological conditions on chest radiographs^{1, 2, 3, 4}. These systems usually employ a two-step approach. The first stage is the identification of left and right lung field (LF) regions, followed by the textural characterization of lung disease-related patterns using a classification algorithm. Methods for LF segmentation include rule-based schemes, pixel classification methods, and active contour methods². Region-based segmentation techniques such as thresholding, region growing and region-labeling are then used to separate infected LF regions from the background. This classification is performed by extracting textural features from the LF region to capture the inherent tissue texture variability. These features include first order region statistics, gray-level co-occurrence matrices (GLCM), wavelet-based features, and geometric fractal dimension (FD)³. In the work of Tolouee et al.⁴ the authors classify four kinds of lung tissue patterns (ground glass, honey combing, reticular, and normal) on high-resolution CT images using a wavelet-based multi-scale filtering technique. There has also been some prior work on automated detection of pneumoconiosis and tuberculosis using support vector machines, artificial neural networks, and ensemble methods^{5, 6, 7, 8}.

Here, we describe our preliminary investigations for deriving and characterizing coarse-level textural regions present in the lung field using an unsupervised segmentation method followed by region characterization. Our work is different

from other previous studies because we derive features from automatically computed lung field regions on chest radiographs instead of entire lung fields. We perform labeling and characterization of lung field regions on a publicly available database from the Japanese Society of Radiological Technology (JSRT)⁹. In the future, feature selection and classification will be performed to identify pathological conditions on chest radiographs. The paper is organized as follows: we first present the unsupervised segmentation methodology, followed by a description of the extracted region-based features. We then provide the results section that describes the segmentation outcome on sample chest radiographs, and region characterization. Our conclusion includes a brief description of planned future work.

2. METHOD

2.1 Background: Cellular automata

Cellular automata (CA) are dynamic systems that evolve on a discrete grid of cells that interact locally to produce information at a global scale¹⁰. In general, any discrete system undergoing deterministic local interactions can be modeled as a cellular automaton. Cellular automaton computation is considered to be “brain-like” and modeled on computations performed by neurons in the human visual cortex. In a CA the value of each cell is based on the values of its neighborhood cells, and is determined according to a set of pre-defined state transition rules. The *state transition function* defines the state of the central pixel at time $t+1$ with respect to the values of cells in its neighborhood at the previous time-point t . Although each cell has an extremely limited view of the whole system, localized information is propagated at each time step, enabling an emergent characteristic at a global level. For example, in case of image segmentation, the state transition rules are applied iteratively to update the value of each pixel in an image to automatically determine homogeneous regions present in an image.

2.2 Segmentation using Unsupervised Grow-Cut

The unsupervised grow-cut method¹¹ is motivated by benefits offered by the *interactive grow-cut algorithm*¹² which offers reasonably robust segmentation, but is dependent on user input and limited by the number of classes defined in the interaction. Starting from user-labeled pixels, the interactive grow-cut algorithm derives an optimal cut (or segmentation) for a given image using pixel-based features. However the outcome of the algorithm is dependent on the correctness of user-marked labels. Therefore, we have developed the *unsupervised grow-cut (UGC) algorithm*, which can automatically identify the number of classes and the class boundaries based on local image features present in an image. Starting from a random number of seed points, the algorithm converges to a natural segmentation of an image. The unsupervised grow-cut algorithm (UGC) incorporates a CA-based framework using low-level image features such as pixel intensity values to derive state-transition rules. Both von Neumann (4-connected) or Moore (8-connected), neighborhoods may be defined for a two-dimensional cellular automaton. As mentioned in the previous section, the state transition function defines the state of the central cell at time $t+1$ with respect to the values of cells in its neighborhood at time t .

The initial labels and the number of seed points are assigned randomly from the space of positive integer values. The state of each cell (pixel) is given by a 3-tuple (l, θ, I) , where l is the label, $\theta \in [0,1]$ is the strength of the cell and I is the pixel intensity value. The strength of a cell is a function of image features and is used to define the state transition function for updating the labels of cells at each time step. Pixels with initial random labels are assigned the cell strength 1. The state transition rule between two pixels p and q is defined using a monotonically decreasing function g as:

$$g(|I_p - I_q|) \cdot \theta_q > t, \quad \text{where,} \quad g(x) = 1 - \left(\frac{x}{\max |I|} \right). \quad (1)$$

In addition, equivalence classes are constructed corresponding to each label; these are updated when two labels merge. The algorithm iterates until the local label update stops occurring. For a given image \mathbf{X} , the equivalence class for pixels p with labels l is defined as:

$$[l] = \{p \in \mathbf{X} \mid p \sim l\}. \quad (2)$$

Thus, the number of desired partitions does not have to be specified by the user before performing segmentation. Also, since the UGC algorithm is dependent on state transitions occurring at local neighborhoods, the computational complexity is independent of the image size or dimension of the feature space. The UGC is particularly useful for this application because:

1. The algorithm converges to a natural segmentation of an image by deriving local homogeneous regions. This is an advantage because the location and spread of disease need not be specified using marker points or user-interaction.
2. The algorithm is extensible to other features. Currently pixel intensity values and Gabor texture features have been used to derive coarse regions from lung fields, but other image features could be easily incorporated into this framework to derive subtle lung disease patterns.

2.3 Region Characterization

Region characterization is performed by deriving region-based features from the coarse-level regions obtained from the segmentation stage. We implement region characterization using Matlab[®] functions. Matlab contains a number of different functions such as *regionprops*, *statmoments*, and *statxture* for computing statistical and geometrical image features. We used the *regionprops* function to compute geometrical and pixel-value features from the lung fields on the radiographs. Below, we discuss the specific region-based features that we derived using *regionprops*.

2.3.1 Geometrical features

We derived four types of geometrical features: *area*, *perimeter*, *extent*, and *orientation* from the segmented regions. The *area* is a scalar value of the number of pixels in a particular region. The *perimeter* is computed by summing the distance between each neighboring pixel along the boundary of a region. The *extent* specifies the ratio of the pixels in the region to the total number of pixels in the bounding box containing the region. The *orientation* is an angle between -90° to 90° measured from the positive x-axis and the major axis of the ellipse with the same second-moment as the region.

2.3.2 Pixel-value measurements

We also derived three types of pixel-value measurements: *maximum intensity*, *minimum intensity*, and *mean intensity* from the segmented lung fields. *Maximum (minimum) intensity* is the value of the pixel with the highest (lowest) intensity in the specified region. *Mean intensity* is the mean value of all intensity values in a given region.

3. DATASET

We segmented a subset of 40 images (20 normal versus lung cancer patients of each gender) taken from the publicly available data set of 247 posterior-anterior-(PA) chest radiographs made publicly available from the Japanese Society of Radiological Technology (JSRT)⁹. The images are 2048x2048 pixels, with a spatial resolution of 0.175 mm/pixel. Of the 247 images, 154 contain one pulmonary nodule each, while the remaining 93 images contain no nodules. Figure 1 shows two images from the dataset, one from a patient with lung cancer containing a nodule (left panel), and the other from a normal person (right panel).

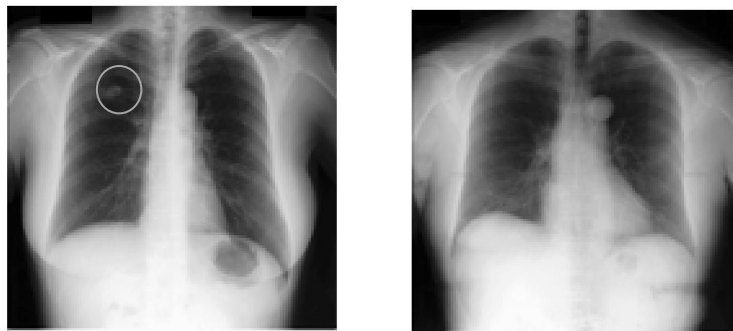


Figure 1. (Left) Chest radiograph of a lung cancer patient with a nodule in the right upper lobe as shown. (Right) Normal chest radiograph.

4. RESULTS AND DISCUSSION

Before segmentation was performed, the images were resized to 512x512 pixels and contrast enhanced using histogram equalization. The resizing was performed so that the coarse-level regions could be derived using fewer number of original seed points, thereby reducing the computational time. Figure 2 shows a sample chest radiograph, randomly assigned initial seed points and the segmentation outcome. Figure 3 shows the segmentation on four sample chest radiographs using the unsupervised grow-cut method. Here, the automatically segmented image is shown superimposed on manually segmented lung fields to depict the extent of segmentation overlap and the various homogeneous regions derived from the lung fields. We computed a 75% segmentation overlap between the automatic segmentation outcome and manual segmentations (from Ginneken et al.²). This was expected because the algorithm does not use any shape-based priors to derive the outline of the lung field. Our goal was to derive homogeneous regions from the lungs by directly targeting relevant textural areas in the chest radiographs, thereby eliminating the stage requiring the delineation of the entire LF boundary. The UGC is useful for our purposes because, it derives the natural boundaries of regions present in chest radiographs without user interaction. The different textural regions may indicate the presence of lung disease patterns such as the presence of nodules from lung cancer; regions of diffuse opacity, and shape abnormality from pleural effusion in pulmonary tuberculosis (TB); and granular patterns in Miliary TB. The next steps in the project are feature selection to characterize such suspicious regions on LFs and developing a robust classifier.



Figure 2. A sample chest radiographs from the JSRT database, randomly assigned original seed points, and final segmentation outcome. The colors have been assigned randomly and depict the various homogeneous regions in the chest radiograph.

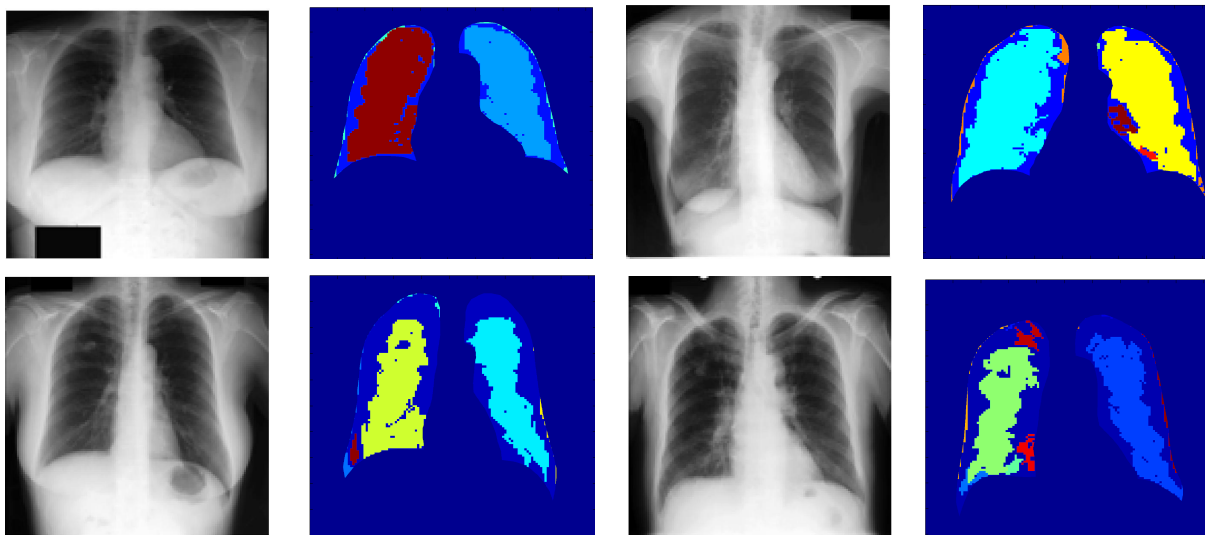


Figure 3. Segmentation outcome from UGC on four chest radiographs from the JSRT database. Segmented images have been shown superimposed on manually derived lung field to depict the various regions found in the lung field. (Top panel) Normal cases; (Lower panel) Lung cancer cases with a nodule in the right lobe. The colors have been assigned randomly and depict the derived textural regions in the LF.

We also derived region-based features from the segmented left and right lung fields using the *regionprops* function in Matlab. The values in Tables 1 and 2 were computed by averaging over normal and lung cancer patients (shown separately for each gender). The lung cancer patients in this subset had a nodule in the right LF. We found that the area and perimeter values computed from right LFs of lung cancer patients to be slightly higher than the normal cases for both male and female subjects. The mean intensity values were also found to be slightly higher for male lung cancer patients, which may be due to the presence of disease patterns. The validation of using these region-based properties along with other statistical features for image classification is a subject for future work.

Table 1. Region-based properties derived from the segmented left and right lung fields (LFs) of normal versus lung cancer patients (averaged over 10 female subjects for each category) using the *regionprops* function in Matlab.

Region Properties		Area	Perimeter	Extent	Orientation	Mean Intensity	Max Intensity	Min Intensity
Normal	Left LF	17070.4±3473.1	864.8±168.5	0.54±0.06	-74.1±4.91	0.19±0.05	0.4±0.13	0.08±0.04
	Right LF	23629±3308.1	1079±142.5	0.62±0.06	79.9±3.6	0.23±0.05	0.53±0.06	0.08±0.04
Lung Cancer	Left LF	20289±1182.3	1167.5±98.4	0.42±0.04	-74.1 ±2.1	0.22±0.04	0.54±0.08	0.08±0.02
	Right LF	24729.6±4744.5	1132±170.3	0.55±0.07	78.0±3.9	0.22±0.03	0.54±0.07	0.08±0.03

Table 2. Region-based properties derived from the segmented left and right lung fields (LFs) of normal versus lung cancer patients (averaged over 10 male subjects for each category) using the *regionprops* function in Matlab.

Region Properties		Area	Perimeter	Extent	Orientation	Mean Intensity	Max Intensity	Min Intensity
Normal	Left LF	23147±5001.5	1179.6±169	0.46±0.07	-72.8±3.27	0.15±0.02	0.46±0.0	0.02±0.01
	Right LF	27577±5316.2	1226.7±235	0.50±0.08	72.8±4.0	0.17±0.04	0.50±0.1	0.03±0.02
Lung Cancer	Left LF	21160±2310.3	1190±140.9	0.4±0.05	-73.5 ±2.4	0.21±0.06	0.55±0.1	0.06±0.03
	Right LF	24745±4038.1	1243±196.2	0.52±0.08	76.9±3.2	0.19±0.04	0.50±0.1	0.05±0.03

5. CONCLUSION

In this paper we present our preliminary analysis of using an unsupervised segmentation method, to automatically derive homogeneous regions within the lung field and to characterize the derived regions by geometric and pixel intensity properties. The unsupervised grow-cut method is particularly useful for this application because it derives the natural boundaries of the regions on the images without user interaction and is extensible. The key difference between our work and prior studies lies in the computation of homogeneous textural regions from lung fields on chest radiographs instead of deriving entire lung fields. Tables 1 and 2 depict examples of region-based features that can be extracted from the derived lung field regions. Geometrical features may be useful for identifying lung diseases that lead to collapsed lungs or other shape abnormalities. In the future, statistical and textural features will be used for characterizing suspicious regions on lung fields such as regions of diffuse opacity that occur in chest x-rays of patients with pulmonary tuberculosis. Feature selection and classification will also be performed to identify such pathological conditions on other chest radiograph datasets.

ACKNOWLEDGEMENTS

This research was supported by the Intramural Research Program of the National Institutes of Health (NIH), National Library of Medicine (NLM), and Lister Hill National Center for Biomedical Communications (LHNCBC).

REFERENCES

- [1] Uppaluri, R., Hoffman, E.A., Sonka, M., Hartley, P. G., Hunninghake, G. W., and McLennan, G., "Computer recognition of regional lung disease patterns," *American Journal of Respiratory and Critical Care Medicine*, 160(2), pp. 648-654 (1999).
- [2] Van Ginneken, B., Katsuragawa, S., Ter Haar Romey, B.M., Doi, K. and Viergever, M.A., "Automatic detection of abnormalities in chest radiographs using local texture analysis," *IEEE Transactions on Medical Imaging*, 21(2), 139-149 (2002).
- [3] Xu, X.W., Doi, K., Kobayashi, T., MacMohan, H., and Giger, M. L., "Development of an improved CAD scheme for automated detection of lung nodules in digital chest images", *Med. Phys.*, 24(9), 1395-1403 (1997).
- [4] Tolouee, A., Abrishami-Moghaddam, H., Garnavi, R., Forouzanfar, M., Giti, M., "Texture analysis in lung HCRT images," *Digital Image Computing: Techniques and Applications*, 305-311 (2008).
- [5] Sundararajan, R., Xu, H., Annangi, P., Tao, X., Sun, X. W., and Mao, L., "A multi resolution support vector machine based algorithm for pneumoconiosis detection from chest radiographs", *Proceedings of the IEEE International Conference on Biomedical imaging*, 1317-1320 (2010).
- [6] Kondo, H. and Kouda, T., "Computer-aided diagnosis for pneumoconiosis using neural network," *Proceedings of IEEE Symposium on Computer-Based Medical Systems*, 467-472 (2001).
- [7] Er, O., Temurtas, F., and Tantrikulu, A. C., "Tuberculosis disease diagnosis using artificial neural networks", *Journal of Medical Systems*, 34(3), 299-302 (2010).
- [8] Asha, T., Natarajan, S. K., Murthy, N. B., "Diagnosis of tuberculosis using ensemble methods," *IEEE International Conference on Computer Science and Information Technology (ICCSIT)*, 8, 409-412 (2010).
- [9] Shirashi, J., Katsuragawa, S., Ikezoe, J., Matsumoto, T., Kobayashi, T., Komatsu, K., Matsui, M., Fujita, H., Kodera, Y. and Doi, K., "Development of a digital image database for chest radiographs with and without a lung nodule: receiver operating characteristic analysis of radiologists' detection of pulmonary nodules", *American Journal of Roentgenology*, 174, 71-74 (2000).
- [10] von Neumann, J., [Theory of Self-Reproducing Automata], Univ. Illinois Press, Urbana, IL (1966).
- [11] Ghosh, P., Antani, S. K., Long, L.R., Thoma, G., "Unsupervised Grow-Cut: Cellular Automata-based Medical Image Segmentation", *IEEE Healthcare Informatics, Imaging, and Systems Biology*, 40-47 (2011).
- [12] Vezhnevets, V. and Konouchine, V., "GrowCut-interactive multi-label ND image segmentation by cellular automata," *Proceedings of Graphicon.*, 231-234 (2006).